Classical molecular dynamics simulations of hypervelocity nanoparticle impacts on amorphous silica

Juha Samela[*] and Kai Nordlund

Department of Physics, University of Helsinki, P.O. Box 43, Helsinki FI-00014, Finland

(Received 26 November 2009; revised manuscript received 19 January 2010; published 12 February 2010)

We have investigated the transition from the atomistic to the macroscopic impact mechanism by simulating large Argon cluster impacts on amorphous silica. The transition occurs at cluster sizes less than 50 000 atoms at hypervelocity regime (22 km/s). After that, the crater volume increases linearly with the cluster size opposite to the nonlinear scaling typical of small cluster impacts. The simulations demonstrate that the molecular dynamics method can be used to explore atomistic mechanisms that lead to damage formation in small particle impacts, for example, in impacts of micrometeorites on spacecraft.

I. INTRODUCTION

Impacts of atomic cluster ions and even single atom ions are often compared to macroscopic impacts like meteorite impacts on planetary surfaces.[1–8] The reason to this is the apparent similarity of the shapes of craters that are observed after both microscopic and macroscopic impacts. However, the mechanisms of crater formation seem to be different in spite the similarity of the final outcomes.[7,9,10] Compression of the impacting body prior to cavity formation is typical to macroscopic impacts.[11,12] The depth and density of the compressed body depends on the properties of materials of the impactor-target system and on the impact velocity. The impact crater is formed when this high-density core expands, rapidly melting and moving material around it. Because of these successive compression and expansion mechanisms, the scaling of the crater volume with the impact mass is linear.[11] In contrast, a characteristic feature of small-scale Atomic cluster impacts is the nonlinear cluster size dependence of crater volume and many other quantities such as sputtering yield.[13–15]

We have recently reported that the transition from the nonlinear scaling behavior typical to the atomic cluster impacts to the linear macroscopic scaling occurs between cluster sizes of 1000–100 000 atoms when Au cluster impacts on the Au(111) surfaces are simulated at velocities typical to the micrometeorite velocities.[9,10] This result arises the question whether the mechanism detected in Au targets occurs also in materials which have a different structure and lower density. In this paper, we show that the mechanism is indeed similar in silicon dioxide (SiO_2) although the response of the material in the expansion phase is different than in Au. Silica is chosen because it represents amorphous materials that are common in nature and important in the applications. Traditionally, cluster and meteorite impacts are described by different theoretical and computational models, and only a few attempts has been made to compare the quantitative scaling laws between nanoscale and macroscopic craters.[1] The increasing performance of parallel computing now provides an opportunity to explore macroscopic impact mechanisms with molecular-dynamics simulations.[16]

The study of transition from microscopic to macroscopic impact mechanism is interesting not only from the basic re-

search point of view. Cluster ion-beam techniques are rapidly developing and can be used to modify surfaces and create nanostructures on surfaces.[8] The knowledge on single impact mechanisms of clusters of various sizes is necessary for understanding of the overall cluster beam irradiation effects. On the other hand, the hypervelocity impact mechanisms are important to understanding of various surface phenomena on planets and moons without atmospheres.[17–19] Micrometeorite impacts are also studied because they are harmful for spacecraft.[20–22]

II. COMPUTER SIMULATIONS

The simulations were carried out using classical molecular dynamics (MD). The simulation arrangements and their suitability for cluster bombardment simulations are discussed in Refs. 23–26. For silica, the Watanabe potential was used in the simulations.[27,28] The potential is specially constructed for silica under a high pressure.

The amorphous silica structures were built of identical copies of a $5 \times 5 \times 2$ nm silica block that was structurally optimized using the algorithm of Wooten, Winer, and Weaire (WWW).[29,30] Before the simulations, the combined structure was annealed in MD to relax possible structural stresses. This method gives a very homogenous silica structure that has bonding characteristics very close to the natural silica. Our tests show that simulated annealing using only MD without the WWW algorithm gives silica structures that are not so well optimized. The density is lower which affects the stopping of the cluster in the material. The sizes of the structures were $100 \times 100 \times 50$ and $150 \times 150 \times 50$ nm. The ambient temperature was 100 K.

Spherical Ar clusters were prepared using a Lennard-Jones potential. Because the binding energies of Ar-Ar, Ar-Si and Ar-O are small compared with those of Si-Si and Si-O, only a repulsive potential was applied to Ar atoms during the simulations.[31] was applied to Ar atoms during the simulations. Cluster sizes were $N = 922$, 7337, 39 315, and 114 534, corresponding to total impact energies $E_{tot} = 0.9$–114.5 MeV.

The length of the simulations and the size of the system was limited by the computer time available. At the longest, one impact simulation took about five days in the parallel
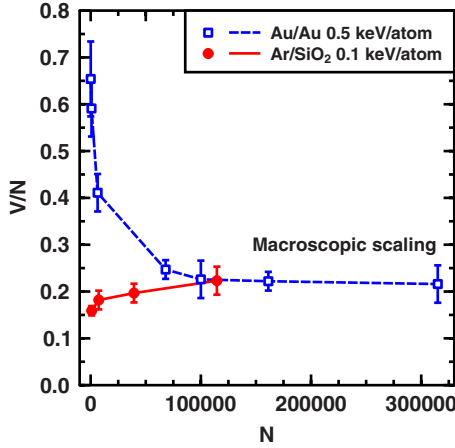
FIG. 1. (Color online) Ratio of crater volume and cluster size V/N as a function of cluster size N. Horizontal line means that the volume increases linearly with the impactor size, which is typical to macroscopic impacts. The values for the Au impact are from Ref. 9.

FIG. 2. (Color online) Crater diameter and depth at different cluster sizes N. Diameter grows faster than depth at large N.

mode using 512 CPUs. Therefore, only the first 20–50 ps after the impacts were simulated. This is enough for crater formation and a good estimate for the crater dimensions can be detected even for the largest cluster impacts in this paper. Possible error in the detected crater dimensions is taken into account in the error estimates.

The velocity of the clusters was chosen to be about 22 km/s (100 eV/atom), which is a typical velocity of small meteorites and allows the comparison to the macroscopic scaling laws concerning hypervelocity impacts. Electronic stopping was applied to atoms having kinetic energy larger than 5 eV.[32–34]

III. RESULTS

In macroscopic impacts, the crater volumes V have empirically been found to follow the behavior

$$V = K_1 \frac{m}{\rho} \left(\frac{\rho U^2}{\bar{Y}} \right)^{3\mu/2}, \qquad (1)$$

where U is the impactor velocity, m is the impactor mass, and ρ is the density of material. $\bar{Y}$, μ, and K_1 are parameters that depend on the strength of the material.[11] We have previously shown[9] for Au cluster impacts on the Au(111) surface that the simulated crater volumes converge toward the estimated macroscopic value $V/N=0.17$ nm³ when the size N of the cluster increases. Figure 1 shows the comparison of the current silica result to this previous result. In both cases, the impact velocity is about 22 km/s. The V/N ratio approaches approximately the same level as the corresponding ratio for Au. However, a clear constant V/N regime is not reached even at the cluster sizes that has been possible in this paper. We can extrapolate from Figs. 1 and 2 that the constant V/N will be reached at $N=300\,000$.

For silica, V/N increases with N at small cluster sizes, whereas the Au system shows an opposite behavior (Fig. 1). In other words, small Au clusters induce craters more efficiently than larger ones. The reason to this is the lower melt-
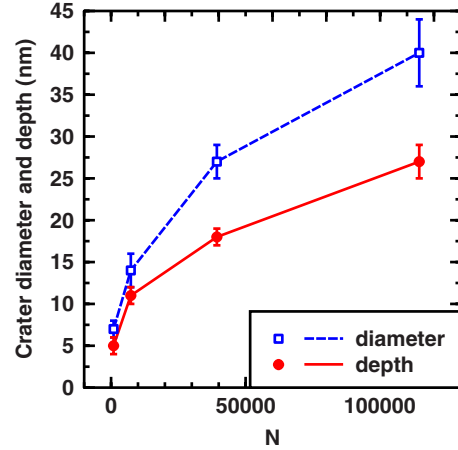
ing point and elasticity of Au compared to the amorphous silica. In Au, small cluster cratering is associated with heat spikes.[35] In silica, the kinetic energy of small clusters does not induce a cavity of melted material as easily as clusters of the same total energy in Au. Figure 1 shows that in both cases, the V/N curves have nonlinear parts at small N and linear (V/N constant) parts at large N. At the linear regime, the crater volume increases linearly with N as it does in macroscopic impacts.

The crater shape changes with N, as shown in Fig. 2. Both diameter and depth still grow at $N=100\,000$, which verifies that the constant regime is not yet reached at the cluster sizes used in these simulations. Diameter grows faster than depth at large N.

Figure 3 shows how the spherical cluster is compressed in a small volume at the first phase of the impact. After that, it expands to form a cavity that becomes a crater by sputtering. These compression and expansion phases are detected also in our previous simulations of Au cluster impacts on the Au(111) surface.[9,10]

The kinetic energy is stored in the compressed cluster. During the expansion phase, the energy is released and it melts a larger region of the material around the expanding cluster. A cavity of Ar, Si, and O mixture gas is formed. The gas sputters out of the cavity. In metals, the mechanism is similar, except that the corona around the crater is larger due to the stronger attraction between the metal atoms.[36,37]

Most of the Ar atoms sputter because the Ar region is surrounded by a melted silica shell at the end of the expansion phase. The crater diameter is about four times larger than the cluster diameter at large N.

The release mechanism of the energy from the compressed core defines the form of structural changes and crater formation. Figure 4 shows that at the early phases, the highest potential-energy density occurs in the shell surrounding the expanding Ar cluster. This energy is consumed in two ways: first, the energy melts material and the cavity of gas is formed. Second, a portion of the energy is deposited over a large volume of the silica structure by a shock wave. The shock wave is strongest parallel to the incident direction of the cluster, and it propagates hemispherically from the cavity.
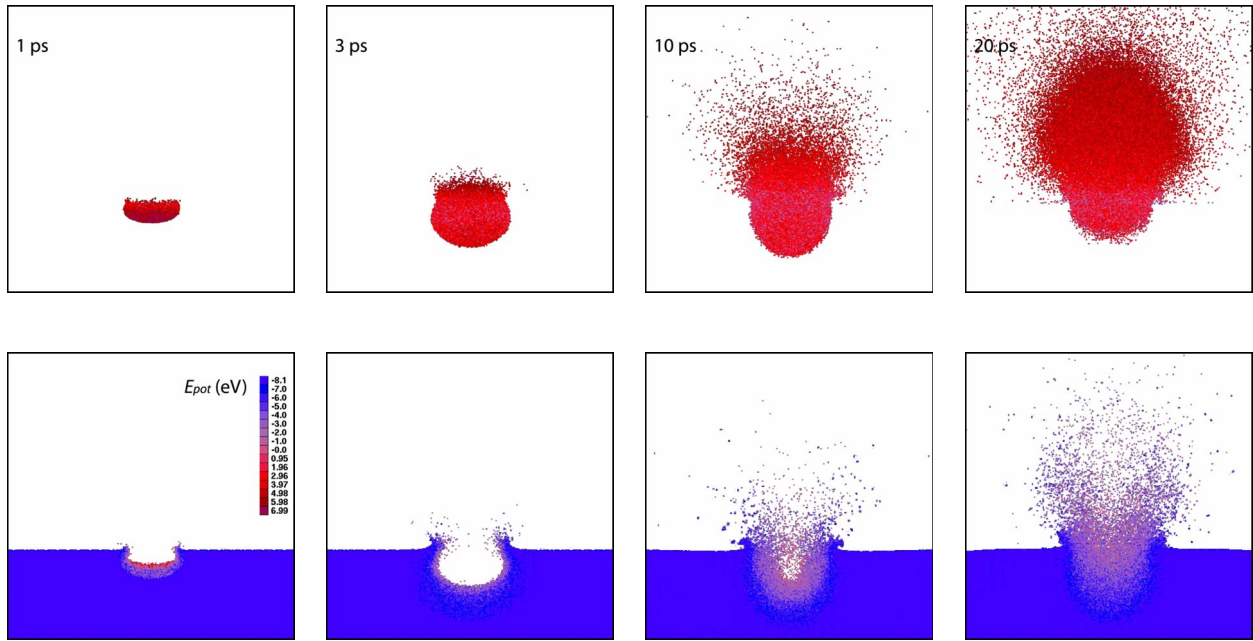
FIG. 3. (Color online) An example of simulated impact of Ar_{114534} cluster onto the silica surface at $E_{kin}=100$ eV/atom. The upper row shows the distribution of Argon atoms at 1–20 ps and the lower row shows the corresponding kinetic energy distributions of Si atoms. The moving Si atoms are marked with shades of red (light gray in printed version). Most of these atoms have kinetic energies less than 1 eV. The frames show 50×50 nm areas and the incident cluster direction is downwards.

IV. DISCUSSION

In silica, we see compression of the impacting cluster similar to the mechanism that was previously detected in crystalline Au.[9] The simulations verify that this two-phase mechanism of crater formation occurs also in silica and is typical not only to dense metallic materials. The pile up of cluster atoms upon impact and formation of the high-density region appears gradually as the cluster size increases. The clear macroscopic behavior is reached at cluster sizes of about 100 000 atoms.

In the theory of planetary impact processes, the impact energy is assumed to be instantaneously deposited in a region of zero extent inside the target.[11] This approximation is valid because the expansion of the energy stored in the compressed region is deposited almost radially in the expansion phase. The simulations in this study and in our previous study[10] show that the high-density region induced by a spherical cluster is rather disk shaped than spherical. However, the zero extent approximation is rather good because most of the potential energy is stored in the bottom of the cavity (Fig. 4) at the beginning of the expansion phase and

the expansion occurs almost radially (Fig. 4). The redirection of the impact momentum to lateral expansion is one of the main characteristics of macroscopic impacts. Figure 2 shows that the width of the crater increases faster than the depth at the transition cluster sizes $N < 50\ 000$. The explanation is that the redirection of the impact momentum to lateral momentum becomes gradually a stronger effect.

The later phases of expansion are different in silica and Au. The liquid flow along the walls of the cavity typical to metallic targets[35,38] is not detected in silica. Instead, the content of the cavity is mostly sputtered direct to the vacuum and only a rather weak liquid flow is detected. The consequence is that the corona is weaker and it does not developed long finger like protrusions.[39] Another consequence is that almost no mixing of the material occurs. The impact just ejects material and a crater is left in the surface. Monoatomic ion beams and small cluster ion beams are used in applications of ion-beam mixing.[40] The results of this paper indicate that large cluster ion beams are not very effective in this task.

The constant V/N as a function cluster size is reached in the Au impact simulations.[9] However, the constant regime is not clearly reached at the present simulations of silica targets
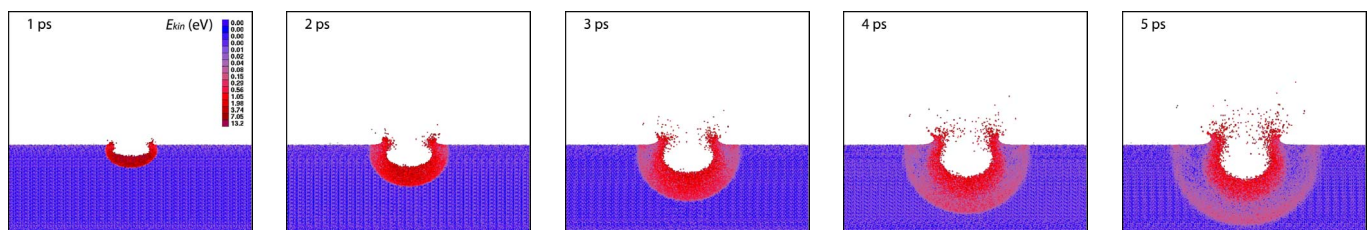

FIG. 4. (Color online) Potential energy distribution of Si atoms at 1, 2, 3, 4, and 5 ps (Ar_{114534}, 100 eV/atom). The atoms that have high potential energy are marked with shades of red (light gray in printed version). The emission of a shock wave is clearly visible at 3–4 ps.

although we observe the impact process typical to the macroscopic impacts. Because of technical reasons, it is not possible to simulate impacts in silica with clusters that are considerably larger than those in the present simulation. Therefore, the question where the constant V/N reached remains open. From the shapes of the curves in Fig. 2 we can extrapolate that the saturation is reached at $N \approx 500\,000$. We have shown for Au that the transition to full macroscopic impact scaling occurs gradually when the impactor size increases.[10] First, the compression process emerges and after that the scaling of crater volume becomes linear at larger cluster sizes. The silica simulations indicate that this transition zone is much wider for silica than it is for Au. In conclusion, we have observed the stopping process to change to macroscopic process in silica but the linear crater scaling is not yet verified to become linear at these cluster sizes.

The shock wave induced in the beginning of the expansion phase (Fig. 4) is rather strong and will induce defects in the material.[16,41] It is well known that impacts induce cracks in glasses.[42] The shock wave observed in this study is strongest in the direction of the incident cluster. It has been shown that the effect of a spherical shock wave is different from a planar shock wave in Ni.[36] Therefore, the possible effects of the shock wave may vary directionally. The most effective method to explore defect and crack formation upon impact will be a two-phase simulation. First, the form and strength of the shock wave is detected from impact simulations. Second, the shock wave is applied to various initial defect configurations. This will help to understand the atomistic mechanisms that cause impact damage in materials with defects and grain boundaries.

Recently, a vanishing electronic stopping power for very slow ions in insulators was observed.[43] However, the threshold kinetic energy where the electronic stopping vanishes for Ar in silica is not known. For smaller clusters and metallic targets, the correct vanishing threshold for the electronic stopping could be important in MD simulations.[34] In our simulations, the electronic stopping was switched off for atoms having kinetic energies less than 5 eV. We expect that this is a reasonable approximation for the threshold, because the electronic stopping does not very much affect the outcome of large cluster impact at this energy regime. The reason is that the Ar atoms penetrate to the substrate as a frontier in both compression and expansion phases, thus relatively small number of Ar atoms travel inside silica.

V. CONCLUSIONS

We have shown that large cluster impacts on silica induce a high-density core that acts as a transient storage of the impact energy. This energy is then released and a crater is formed. The mechanism is the same as that known to occur in macroscopic hypervelocity impacts. The transition from atomistic to macroscopic impact process occur at cluster sizes $N = 1000 - 50\,000$ and the linear scaling of crater volumes with the cluster size is reached probably at $N \approx 500\,000$.

This result and our recent simulations of large Au cluster impacts demonstrate that large-scale atomistic simulations can be used to explore atomistic mechanisms of impacts in a regime that is traditionally studied with means of continuum mechanics. Although it is not yet possible to simulate size and time scales of real micrometeorite impacts with molecular dynamics method, it is now possible to get results which can help to understand these phenomena more deeply.

---

*juha.samela@helsinki.fi

[1] R. Aderjan and H. M. Urbassek, Nucl. Instrum. Methods Phys. Res. B **164-165**, 697 (2000).

[2] K. Nordlund, K. O. E. Henriksson, and J. Keinonen, Appl. Phys. Lett. **79**, 3624 (2001).

[3] E. M. Bringa, E. Hall, R. E. Johnson, and R. M. Papaléo, Nucl. Instrum. Methods Phys. Res. B **193**, 734 (2002).

[4] Y. Yamaguchi, J. Gspann, and T. Inaba, Eur. J. Phys. D **24**, 315 (2003).

[5] V. N. Popok, S. V. Prasalovich, and E. E. B. Campbell, Surf. Sci. **566-568**, 1179 (2004).

[6] R. Papoular, Astron. Astrophys. **414**, 573 (2004).

[7] E. M. Bringa, K. Nordlund, and J. Keinonen, Phys. Rev. B **64**, 235426 (2001).

[8] V. N. Popok and E. E. B. Campbell, Rev. Adv. Mater. Sci. **11**, 19 (2006).

[9] J. Samela and K. Nordlund, Phys. Rev. Lett. **101**, 027601 (2008).

[10] J. Samela and K. Nordlund, Nucl. Instrum. Methods Phys. Res. B **267**, 2980 (2009).

[11] K. A. Holsapple, Annu. Rev. Earth Planet Sci. **21**, 333 (1993).

[12] E. Pierazzo, A. M. Vickery, and H. J. Melosh, Icarus **127**, 408 (1997).

[13] S. Bouneau, A. Brunelle, S. Della-Negra, J. Depauw, D. Jacquet, Y. Le Beyec, M. Pautrat, M. Fallavier, J. C. Poizat, and H. H. Andersen, Phys. Rev. B **65**, 144106 (2002).

[14] R. A. Baragiola, Philos. Trans. R. Soc. London, Ser. A **362**, 29 (2004).

[15] J. Samela and K. Nordlund, Phys. Rev. B **76**, 125434 (2007).

[16] C. Zhang, R. K. Kalia, A. Nakano, and P. Vashishta, Appl. Phys. Lett. **91**, 121911 (2007).

[17] G. G. Managadze, W. B. Brinckerhoff, and A. E. Chumikov, Geophys. Res. Lett. **30**, 1247 (2003).

[18] Y. Futaana, S. Barabash, M. Holmström, and A. Bhardwaj,

Planet. Space Sci. **54**, 132 (2006).

[19] C. F. Chyba, P. J. Thomas, L. Brookshaw, and C. Sagan, Science **249**, 366 (1990).

[20] V. Jantou, D. McPhail, R. Chater, and A. Kearsley, Appl. Surf. Sci. **252**, 7120 (2006).

[21] A. Kearsley and G. Graham, Adv. Space Res. **34**, 939 (2004).

[22] A. Kearsley, G. Graham, J. McDonnell, E. Taylor, G. Drolshagen, R. Chater, D. McPhail, and M. Burchell, Adv. Space Res. **39**, 590 (2007).

[23] G. Kornich, G. Betz, V. Zaporojtchenko, and K. Pugina, Nucl. Instrum. Methods Phys. Res. B **255**, 233 (2007).

[24] J. Samela, J. Kotakoski, K. Nordlund, and J. Keinonen, Nucl. Instrum. Methods Phys. Res. B **239**, 331 (2005).

[25] M. Ghaly, K. Nordlund, and R. S. Averback, Philos. Mag. A **79**, 775 (1999).

[26] K. Nordlund, M. Ghaly, R. S. Averback, M. Caturla, T. Diaz de la Rubia, and J. Tarus, Phys. Rev. B **57**, 7556 (1998).

[27] F. H. Stillinger and T. A. Weber, Phys. Rev. B **31**, 5262 (1985).

[28] F. H. Stillinger and T. A. Weber, Phys. Rev. B **33**, 1451 (1986).

[29] F. Wooten, K. Winer, and D. Weaire, Phys. Rev. Lett. **54**, 1392 (1985).

[30] S. von Alfthan, A. Kuronen, and K. Kaski, Phys. Rev. B **68**, 073203 (2003).

[31] K. Nordlund, N. Runeberg, and D. Sundholm, Nucl. Instrum.

[32] K. Nordlund, Comput. Mater. Sci. **3**, 448 (1995).

[33] J. F. Ziegler, J. P. Biersack, and U. Littmark, *The Stopping and Range of Ions Matter* (Pergamon, New York, 1985).

[34] L. Sandoval and H. M. Urbassek, Phys. Rev. B **79**, 144115 (2009).

[35] M. Ghaly and R. S. Averback, Phys. Rev. Lett. **72**, 364 (1994).

[36] E. V. Esquivel, L. E. Murr, E. A. Trillo, and M. Baquera, J. Mater. Sci. **38**, 2223 (2003).

[37] J. Samela and K. Nordlund, Nucl. Instrum. Methods Phys. Res. B **263**, 375 (2007).

[38] M. M. Jakas, E. M. Bringa, and R. E. Johnson, Phys. Rev. B **65**, 165425 (2002).

[39] K. Nordlund, J. Tarus, J. Keinonen, S. Donnelly, and R. Birtcher, Nucl. Instrum. Methods Phys. Res. B **206**, 189 (2003).

[40] N. Toyoda and I. Yamada, IEEE Trans. Plasma Sci. **36**, 1471 (2008).

[41] C. Zhang, R. K. Kalia, A. Nakano, and P. Vashishta, Appl. Phys. Lett. **91**, 071906 (2007).

[42] T. Fett, G. Rizzi, D. Creek, S. Wagner, J. P. Guin, J. M. López-Cepero, and S. M. Wiederhorn, Phys. Rev. B **77**, 174110 (2008).

[43] S. N. Markin, D. Primetzhofer, and P. Bauer, Phys. Rev. Lett. **103**, 113201 (2009).